The temporal and latitudinal dependences of turbulence driven by pickup ions in the outer heliosphere

Bingbing Wang[1]*, Lingling Zhao[1,2], Paria Abouhamzeh[1,2], Gary P. Zank[1,2] and Laxman Adhikari[1,2]

[1]Center for Space Plasma and Aeronomic Research (CSPAR), University of Alabama in Huntsville, Huntsville, AL, United States, [2]Department of Space Science, University of Alabama in Huntsville, Huntsville, AL, United States
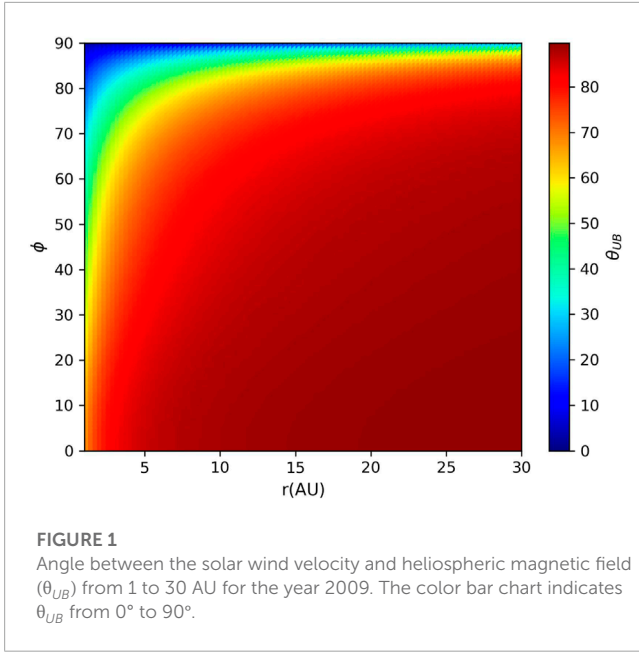
The distribution of turbulence in the heliosphere remains a mystery, due to the complexity in not only modeling the turbulence transport equations but also identifying the drivers of turbulence that vary with time and spatial location. Beyond the ionization cavity (a few astronomical units (AU) from the Sun), the turbulence is driven predominantly by freshly created pickup ions (PUIs), in contrast to the driving by stream shear and compression. Understanding the source characteristics is necessary to refine turbulence transport models and interpret measurements of turbulence and solar wind temperature in the outer heliosphere. Using a recent latitude-dependent solar wind speed model and the ionization rate of neutral interstellar hydrogen (H), we investigate the temporal and spatial variation in the strength of low-frequency turbulence driven by PUIs from 1998 to 2020. We find that the driving rate is stronger during periods of high solar activity and at lower latitudes in the outer heliosphere. The driving rates for parallel and anti-parallel propagating (relative to the background magnetic field) slab turbulence have different spatial and latitude dependences. The calculated generation rate of turbulence by PUIs is an essential ingredient to investigate the latitude dependence of turbulence in the outer heliosphere, which is important to understand the heating of the distant solar wind and the modulation of cosmic rays.

KEYWORDS

magnetohydrodynamic turbulence, heliosphere, solar wind, waves and instabilities, pickup ions

1 Introduction

Although turbulence plays a crucial role in multiple aspects of space physics and astrophysics, the distribution of turbulence in our solar system remains unclear, especially in the outer heliosphere, which has been explored by few spacecraft. Many models have been developed over the past few decades to describe the transport of turbulence in the heliosphere (Breech et al., 2008; Ng et al., 2010; Oughton et al., 2011; Usmanov et al., 2011; Zank et al., 2012; 2017; 2018; Nakanotani et al., 2020; Wang et al., 2022; Adhikari et al., 2023), and the source terms that describe the driving of turbulence are indispensable. Due to uncertainty in the model parameters, oversimplified source terms, and a lack of observations, a consensus has not been reached yet about the overall model, and consequently, different models coexist.

FIGURE 1
Angle between the solar wind velocity and heliospheric magnetic field (θ_{UB}) from 1 to 30 AU for the year 2009. The color bar chart indicates θ_{UB} from 0° to 90°.

In this work, we investigated the temporal and latitudinal evolution of turbulence driven by pickup ions (PUIs). Beyond the ionization cavity for neutral hydrogen, turbulence is mainly driven by PUIs. The newborn PUIs initially form a ring-beam distribution, which is highly unstable and drives electromagnetic fluctuations. The energy transferred from PUIs to turbulence is free energy. The driving rate of turbulence by PUIs is the product of the free energy of a single PUI and the creation rate of PUIs. The latter is also closely related to solar activity and depends on latitude. To calculate the driving rate of turbulence by PUIs, we adopt the solar wind speed model derived from remote observations via interplanetary scintillations (IPSs). The heliospheric magnetic field measured by the ACE spacecraft in the ecliptic plane is used as the input for the Parker magnetic field model to obtain the magnetic field within the termination shock. The observation-based solar wind and extreme ultraviolet radiation data provide the ionization rates as a function of time and latitude. We investigate the evolution of the turbulence driving rate by PUIs (i.e., the source of turbulence due to PUIs) from 1998 to 2020.

2 Methods and results

In the outer heliosphere, beyond the ionization cavity, freshly created pickup ions are the main source of turbulence (Zank et al., 1996). The amplification of turbulence/waves due to newborn pickup ions is observed by multiple spacecraft (Smith et al., 2017; Sokół et al., 2022). The driving rate of the turbulence is given by Zank et al. (1996) as follows:

$$\frac{dE}{dt} = \frac{\mathrm{d}n_{PUI}}{\mathrm{d}t} U^2 \times \left(\frac{v_A}{U} \right), \qquad (1)$$

where $n_{PUI(SW)}$ is the pickup ion (solar wind) density, $\mathrm{d}n_{PUI}/\mathrm{d}t = n_a\beta$ denotes the production rate of pickup ions, U is the solar wind speed, and v_A is the Alfvén speed. n_a is the density of neutral H

atoms, and β is the ionization rate. The factor v_A/U represents the fraction of pickup ion kinetic energy available for the generation of turbulence (the so-called free energy) (Lee and Ip, 1987; Huddleston and Johnstone, 1992; Williams and Zank, 1994). Although this fraction gives the correct free energy for most of the heliospheric region where the solar wind velocity is perpendicular to the heliospheric magnetic field, the free energy for the slab turbulence that propagates parallel (E^+) and anti-parallel (E^-) relative to the large-scale magnetic field is generally different and depends on the angle between the solar wind velocity and large-scale magnetic field (θ_{UB}) (Williams and Zank, 1994)[1].

$$E^+ = n_{PUI}mv_A \frac{2\pi v_+}{a_T} \left[\frac{1}{2}(v_+ - v_A)^2 + U_\parallel \left(\frac{U_\parallel}{2} + v_A - v_+ \right) \right]; \qquad (2)$$

$$E^- = n_{PUI}mv_A \frac{2\pi v_-}{a_T} \left[\frac{1}{2}(v_- - v_A)^2 + U_\parallel \left(\frac{U_\parallel}{2} + v_- - v_A \right) \right], \qquad (3)$$

where $v_\pm^2 = U_\perp^2 + (U_\parallel \pm v_A)^2$ and $a_T = 2\pi[v_+^2 + v_-^2 - v_+(U_\parallel + v_A) + v_-(U_\parallel - v_A)]$. $U_\parallel = U\cos(\theta_{UB})$ is the solar wind speed parallel to the magnetic field, and $\cos(\theta_{UB})$ is given by

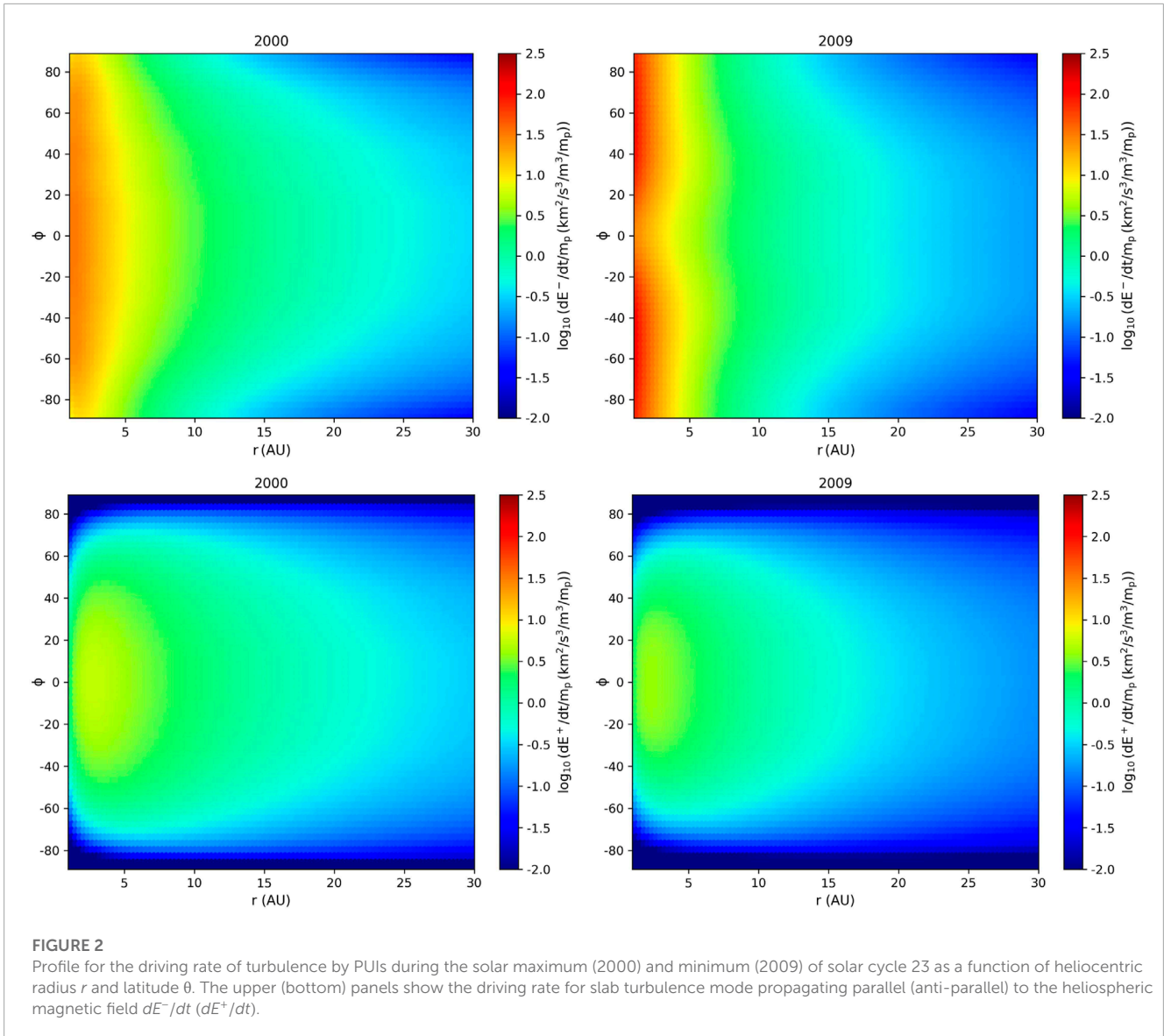$$\cos(\theta_{UB}) = \frac{B_r}{\sqrt{1 + \gamma^2(r, \theta)}}, \qquad (4)$$

where $\gamma = r\Omega \sin(\theta)/U$ and Ω is the angular frequency of the solar rotation. The three fast latitude scans of Ulysses measured the solar wind speed out of the ecliptic plane, covering nearly the entire range of solar latitudes in a relatively short time (07/94–08/95, 11/2000–10/2001, and 02/2007–02/2008) (McComas et al., 2002). During the first and third scans around the solar minimum, Ulysses observed a well-ordered solar wind structure, and the solar wind speed increased from ~400 km s⁻¹ at low latitudes to ~800 km s⁻¹ at high latitudes (McComas et al., 2000). Ulysses' second fast latitude scan, near the solar maximum, found an irregularly structured mixture of slow and intermediate speed flows (McComas et al., 2002). The structure of the solar wind speed during periods of moderate solar activity is unclear due to the lack of direct observations. To investigate the time and latitude dependence of the turbulence driving rate by PUIs, indirect measurements of the solar wind speed are needed. In this work, we adopt the latest solar wind speed model, which is based on remote observations via interplanetary scintillations (IPSs). The solar wind speed is inferred as a function of latitude based on the study of the delay time of the measured scintillation pattern of the radio signal between stations (Sokół et al., 2020). The simple analytic formula based on Legendre polynomials proposed by Porowski et al. (2022) is adopted to model the latitudinal profiles of the solar wind speed at 1 AU (U_1).

$$U_1(\theta) = \sum_0^N Q_i P_i(z), \qquad z = \cos(\theta), \qquad (5)$$

where P_i is the Legendre polynomial of ith order, Q_i is the coefficient of ith polynomial, and N is the order. The coefficients are listed

---

1 We note that there are typos in the equations for free energy given by Huddleston and Johnstone (1992), Eqs 27, 28. The correct expressions should be $E_{F,u} = 0.5m_i n_u [V_A V_u^2 \sin^2(\theta_u)/(V_u + u\cos(\alpha) - V_A) + 2uV_A\cos(\alpha) - 2V_A^2]$ and $E_{F,d} = 0.5m_i n_d [V_A V_d^2 \sin^2(\theta_d)/(V_d - u\cos(\alpha) - V_A) + 2uV_A\cos(\alpha) - 2V_A^2]$.

FIGURE 2
Profile for the driving rate of turbulence by PUIs during the solar maximum (2000) and minimum (2009) of solar cycle 23 as a function of heliocentric radius r and latitude θ. The upper (bottom) panels show the driving rate for slab turbulence mode propagating parallel (anti-parallel) to the heliospheric magnetic field dE^-/dt (dE^+/dt).

in Table 2. The deceleration of the solar wind speed in the outer heliosphere by PUIs is modeled as (Isenberg et al., 2010)

$$U(r,\theta) = U_1(\theta) - 1.4 \times (r - 18), \ r \geq 18 \ \text{AU}; \tag{6}$$

$$= U_1(\theta) \ r < 18 \ \text{AU}, \tag{7}$$

where U is measured in the units of km s^{-1} and r is measured in the units of AU.

For the heliospheric magnetic field, we use the Parker magnetic field model (Parker, 1958):

$$\mathbf{B} = \frac{B_0}{r^2} \left(\mathbf{e}_r - \gamma \mathbf{e}_\phi \right), \tag{8}$$

where B_0 is a constant. The magnetic field in the elliptic plane is measured by the ACE spacecraft and can be obtained from the ACE Science Center[2]. With the solar wind speed and the heliospheric
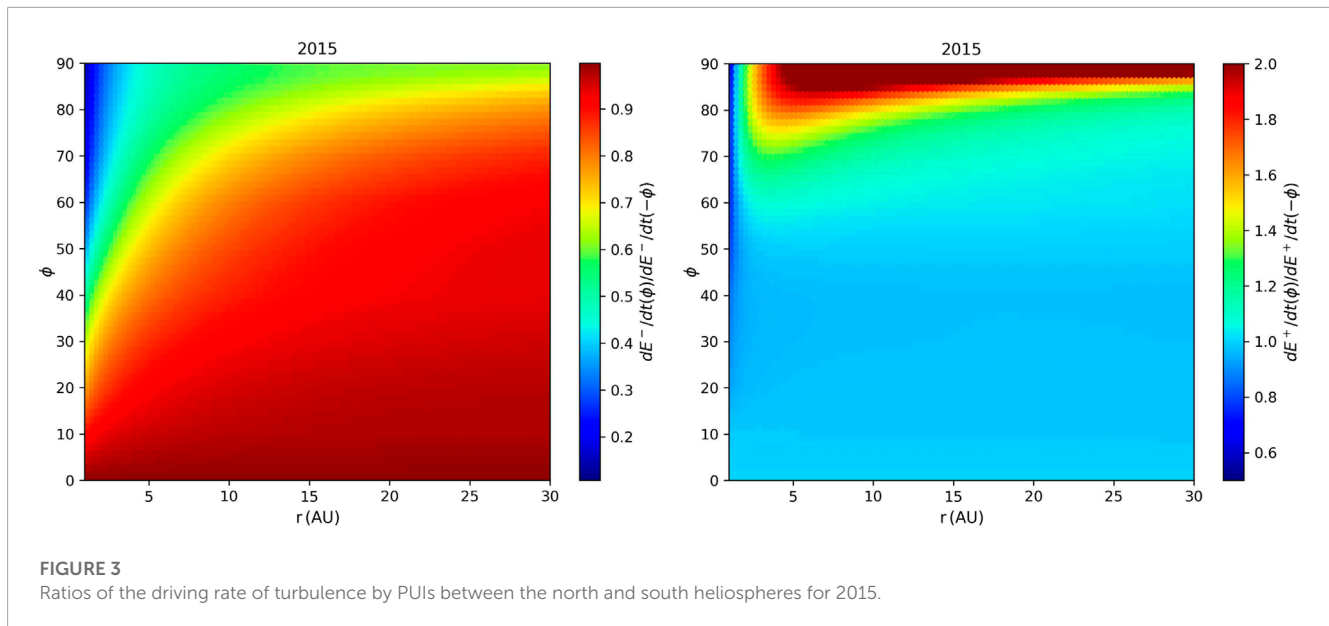
___

2 https://izw1.caltech.edu/ACE/ASC.

magnetic field, we can calculate their angle, θ_{UB}. As shown in Figure 1, in the inner heliosphere and at high latitudes, θ_{UB} is not as large as 90°, and thus, the more general Eqs 2, 3 are needed to accurately describe the free energies.

To obtain the Alfvén speed for Eqs 2, 3, we further need the profile of the plasma density. The solar wind speed and density are linked through the solar wind energy flux, and the energy flux is independent of the latitude within a factor of 10% (Le Chat et al., 2012). The latitude-dependent density at 1 AU ($\rho_1(\theta)$) can be derived via (Le Chat et al., 2012)

$$W\left[\text{W m}^2\right] = \rho_1(\theta) U_1(\theta) \left(\frac{1}{2} U_1(\theta)^2 + \frac{GM_s}{R_s} \right)$$

$$= \rho_E U_E \left(\frac{1}{2} U_E^2 + \frac{GM_s}{R_s} \right), \tag{9}$$

where $U_E = U (r = 1\text{AU}, \theta = \pi/2)$, ρ_E/m_p is the measured solar wind proton density near Earth (m_p is the proton mass), G is the gravitational constant, M_s is the mass of the Sun, and R_s is the radius of the Sun. We use the yearly averaged values to calculate

FIGURE 3
Ratios of the driving rate of turbulence by PUIs between the north and south heliospheres for 2015.

$\rho(\theta)$. According to the mass continuity equation, the density in the outer heliosphere is $\rho(r,\theta) = \rho_1(\theta)\left(\frac{1\,\text{AU}}{r}\right)^2 \frac{U_1(\theta)}{U(r,\theta)}$. For more detailed models, taking into account α particles in the plasma density (the yearly averaged ratio of the number density between α particles and protons from 1998 to 2020 measured by the ACE spacecraft is within the range of 0.0173–0.0417), we refer the readers to Le Chat et al. (2012) Sokół et al. (2020); Porowski et al. (2022). The Alfvén speed $\left(= 21.8\left(\frac{B}{\text{nT}}\right)/\sqrt{\frac{\rho}{m_p\,cm^{-3}}}\,\text{km s}^{-1}\right)$ in Eqs 2, 3 introduces a strong latitudinal dependence. For $\theta \to 0$, V_A is $\propto 1/r$, but for $\theta \to \pi/2$ or $r \gg 1$, V_A approaches a constant $V_{A0}r_0\Omega/U$. Thus, the newborn pickup ions can effectively amplify turbulence at low and middle latitudes, but they scarcely drive the turbulence over the poles in the outer heliosphere.

The driving rate is proportional to the creation rate of PUIs, $dE^{\pm}/dt \propto \frac{dn_{PUI}}{dt} = n_a\beta$. Under the assumption that the neutrals constitute a unidirectional flow (a "cold" gas), particularly in cases where solar radiation pressure equals gravity, which may be applicable during low solar activity levels (Thomas, 1978; Nakanotani et al., 2020), the distribution of the density of the neutral atoms is (see Thomas, 1978; Zank et al., 2022, and references therein).

$$n_a = n_{a,TS} \exp\left(-\frac{\lambda\theta'}{r\sin(\theta')}\right), \tag{10}$$

where $\lambda \equiv \beta_1 r_0^2/U_a$ is the length of the ionization cavity, β_1 is the ionization rate at 1 AU, and $U_a \approx 25$ km s^{-1} is the bulk speed of neutral atoms relative to the Sun. Here, θ' is the angle distance from the upwind direction. Since $\theta' = |\theta - \pi/2|$, it corresponds to the heliospheric latitude for the upwind region. In this work, we treat the neutral H density at the termination shock ($n_{a,TS}$) as a latitude-independent constant ($= 0.127$ cm^{-3} (Swaczyna et al., 2020)) for simplification. Nonetheless, due to the elongation of the heliosphere, the density of the H wall located between the heliopause and the bow shock is maximum in the ecliptic plane, i.e., neutral H is filtrated

more effectively in the ecliptic plane, and thus, less interstellar H can be expected to flow into the heliosheath in the ecliptic plane compared to over the poles, despite the small difference in H density at the termination shock(Pauls and Zank, 1996; Pauls and Zank, 1997). The distribution of neutral atoms is symmetric with respect to the direction of upwind interstellar flow.

The ionization rate changes with latitude and solar activity cycle as a result of variation in the solar wind flow and the solar extreme ultraviolet (EUV) flux (Bzowski et al., 2013; Sokół et al., 2019; Sokół et al., 2020). The dominant ionization process for H atoms is the charge exchange with solar wind particles. The resulting ionization rate is equal to the product of solar wind (number) density, the relative speed between H atoms and solar wind speed, and the cross section as a function of relative speed. As the latitude dependence of the solar wind speed is derived from the fact that the energy flux of the solar wind is almost latitude-independent, the product of solar wind density and solar wind speed is approximately inversely proportional to the square of the solar wind speed, and the cross section decreases with an increase in solar wind speed (Barnett et al., 1990; Lindsay and Stebbings, 2005; Wang et al., 2023). Therefore, a higher solar wind speed leads to a smaller ionization rate and *vice versa*. Obviously, the ionization rate is closely related to latitude and the solar cycle. In this work, we use the data for the total ionization rate (sum of charge exchange, photoionization, and electron impact ionization) for H atoms from Sokół et al. (2020) based on the solar wind and solar EUV data.

The profiles of the driving rate ($dE^{\pm}/dt$) of turbulence due to the creation of PUIs are shown in Figure 2 for 2000 and 2009, corresponding to the solar maximum and minimum of solar cycle 23. $dE^{\pm}/dt$ decreases with an increase in distance and strongly depends on latitude. At the solar minimum and within ~5 AU from the Sun, dE^{-}/dt is larger at intermediate and high latitudes than at low latitudes due to a higher solar wind speed (i.e., PUI kinetic energy), although the ionization rate is weaker. When the solar wind

speed becomes nearly uniform at the solar maximum, the latitudinal dependence of the ionization rate becomes important, and thus, dE^-/dt is larger at low latitudes. A small θ_{UB} value at high latitudes results in a large E^- (and E^+) value. This effect only plays a minor role in determining the latitudinal dependence of dE^-/dt. However, E^+ decreases quickly with an increase in θ_{UB} at high latitudes; therefore, dE^+/dt is large at low latitudes. In the outer heliosphere, θ_{UB} approaches 90° for most of the region except near the poles, which leads to the difference between E^- and E^+ becoming smaller for different latitudes, correspondingly $dE^-/dt \approx dE^+/dt$. Comparing the left and right panels, we can see that $dE^\pm/dt$ is larger at the solar maximum than at the solar minimum in the outer heliosphere. Yearly $dE^\pm/dt$ from 1998 to 2020 is illustrated in the Supplementary Material. As illustrated in Figure 3, the driving rates present a strong north–south asymmetry due to the asymmetric solar wind speed, especially near the solar maximum, and these differences change with latitude and radial distance.

3 Conclusion

Turbulence in the outer heliosphere is predominantly driven by freshly created pickup ions. The resulting generation rate of turbulence energy depends on the solar wind speed, Alfvén speed, magnetic field-flow geometry, neutral density, and ionization rate. Using the latest latitudinal-dependent solar wind speed model inferred from the remote IPS observations, a comprehensive investigation of the ionization rate model, and the Parker magnetic field model inferred from the measurements by the ACE spacecraft, we calculated the yearly rate of turbulence energy generated by PUIs from 1998 to 2020. We found that the driving rate significantly changes with the solar cycle and latitude. In the outer heliosphere, the driving rate increases with the level of solar activity and decreases with an increase in the latitude. Our work shows that it is inappropriate to treat PUI-driven source terms in turbulence transport models as time-independent and latitude-independent (Adhikari et al., 2014). Improving the source term in turbulence transport models is important for understanding phenomena such as the heating of the solar wind (Matthaeus et al., 1999) and the scatting of cosmic rays (Zank et al., 1998; Zhao et al., 2018).

Data availability statement

The raw data supporting the conclusion of this article will be made available by the authors, without undue reservation.

Author contributions

BW: writing–original draft. LZ: writing–review and editing. PA: writing–review and editing. GZ: writing–review and editing. LA: writing–review and editing.

Funding

Acknowledgments

Conflict of interest

The authors declare that the research was conducted in the absence of any commercial or financial relationships that could be construed as a potential conflict of interest.

Publisher's note

All claims expressed in this article are solely those of the authors and do not necessarily represent those of their affiliated organizations, or those of the publisher, the editors, and the reviewers. Any product that may be evaluated in this article, or claim that may be made by its manufacturer, is not guaranteed or endorsed by the publisher.

Supplementary material

The Supplementary Material for this article can be found online at: https://www.frontiersin.org/articles/10.3389/fspas.2023.1298577/full#supplementary-material

References

Adhikari, L., Zank, G. P., Hu, Q., and Dosch, A. (2014). Turbulence transport modeling of the temporal outer heliosphere. *ApJ* 793, 52. doi:10.1088/0004-637X/793/1/52

Adhikari, L., Zank, G. P., Wang, B., Zhao, L., Telloni, D., Pitna, A., et al. (2023). Theory and transport of nearly incompressible magnetohydrodynamic turbulence: high plasma beta regime. *ApJ* 953, 44. doi:10.3847/1538-4357/835/2/147

Barnett, C. F., Hunter, H. T., Fitzpatrick, M. I., Alvarez, I., Cisneros, C., and Phaneuf, R. A. (1990). "Atomic data for fusion," in *Volume 1: collisions of H, H2, He and Li atoms and ions with atoms and molecules.*

Breech, B., Matthaeus, W. H., Minnie, J., Bieber, J. W., Oughton, S., Smith, C. W., et al. (2008). Turbulence transport throughout the heliosphere. *J. Geophys. Res. (Space Phys.* 113, A08105. doi:10.1029/2007JA012711

Bzowski, M., Sokół, J. M., Tokumaru, M., Fujiki, K., Quémerais, E., Lallement, R., et al. (2013). "Solar parameters for modeling the interplanetary background," in *Cross-calibration of far UV spectra of solar system objects and the heliosphere*. Editors E. Quémerais, M. Snow, and R.-M. Bonnet (New York, NY: Springer), 67. doi:10.1007/978-1-4614-6384-9_3

Huddleston, D. E., and Johnstone, A. D. (1992). Relationship between wave energy and free energy from pickup ions in the Comet Halley Environment. *J. Geophys. Res.* 97, 12217–12230. doi:10.1029/92JA00726

Isenberg, P. A., Smith, C. W., Matthaeus, W. H., and Richardson, J. D. (2010). Turbulent heating of the distant solar wind by interstellar pickup protons in a decelerating flow. *ApJ* 719, 716–721. doi:10.1088/0004-637X/719/1/716

Le Chat, G., Issautier, K., and Meyer-Vernet, N. (2012). The solar wind energy flux. *Sol. Phys.* 279, 197–205. doi:10.1007/s11207-012-9967-y

Lee, M. A., and Ip, W. H. (1987). Hydromagnetic wave excitation by ionized interstellar hydrogen and helium in the solar wind. *J. Geophys. Res.* 92, 11041–11052. doi:10.1029/JA092iA10p11041

Lindsay, B. G., and Stebbings, R. F. (2005). Charge transfer cross sections for energetic neutral atom data analysis. *J. Geophys. Res. (Space Phys.* 110, A12213. doi:10.1029/2005JA011298

Matthaeus, W. H., Zank, G. P., Smith, C. W., and Oughton, S. (1999). Turbulence, spatial transport, and heating of the solar wind. *Phys. Rev. Lett.* 82, 3444–3447. doi:10.1103/PhysRevLett.82.3444

McComas, D. J., Barraclough, B. L., Funsten, H. O., Gosling, J. T., Santiago-Muñoz, E., Skoug, R. M., et al. (2000). Solar wind observations over Ulysses' first full polar orbit. *J. Geophys. Res.* 105, 10419–10434. doi:10.1029/1999JA000383

McComas, D. J., Elliott, H. A., Gosling, J. T., Reisenfeld, D. B., Skoug, R. M., Goldstein, B. E., et al. (2002). Ulysses' second fast-latitude scan: complexity near solar maximum and the reformation of polar coronal holes. *Geophys. Res. Lett.* 29, 1290. doi:10.1029/2001GL014164

Nakanotani, M., Zank, G. P., Adhikari, L., Zhao, L. L., Giacalone, J., Opher, M., et al. (2020). The downwind solar wind: model comparison with pioneer 10 observations. *ApJ* 901, L23. doi:10.3847/2041-8213/abb81e

Ng, C. S., Bhattacharjee, A., Munsi, D., Isenberg, P. A., and Smith, C. W. (2010). Kolmogorov versus Iroshnikov-Kraichnan spectra: consequences for ion heating in the solar wind. *J. Geophys. Res. (Space Phys.* 115, A02101. doi:10.1029/2009JA014377

Oughton, S., Matthaeus, W. H., Smith, C. W., Breech, B., and Isenberg, P. A. (2011). Transport of solar wind fluctuations: a two-component model. *J. Geophys. Res. (Space Phys.* 116, A08105. doi:10.1029/2010JA016365

Parker, E. N. (1958). Dynamics of the interplanetary gas and magnetic fields. *ApJ* 128, 664. doi:10.1086/146579

Pauls, H. L., and Zank, G. P. (1996). Interaction of a nonuniform solar wind with the local interstellar medium. *J. Geophys. Res.* 101, 17081–17092. doi:10.1029/96JA01298

Pauls, H. L., and Zank, G. P. (1997). Interaction of a nonuniform solar wind with the local interstellar medium 2. A two-fluid model. *J. Geophys. Res.* 102, 19779. doi:10.1029/97JA01716

Porowski, C., Bzowski, M., and Tokumaru, M. (2022). A New 3D solar wind speed and density model based on interplanetary scintillation. *ApJS* 259, 2. doi:10.3847/1538-4365/ac35d7

Smith, C. W., Aggarwal, P., Argall, M. R., Burlaga, L. F., Bzowski, M., Cannon, B. E., et al. (2017). Observations of low-frequency magnetic waves due to newborn interstellar pickup ions using ace, ulysses, and voyager data. *J. Phys. Conf. Ser.* 900, 012018. doi:10.1088/1742-6596/900/1/012018

Sokół, J. M., Bzowski, M., and Tokumaru, M. (2019). Interstellar neutral gas species and their pickup ions inside the heliospheric termination shock. Ionization rates for H, O, Ne, and He. *ApJ* 872, 57. doi:10.3847/1538-4357/aafdaf

Sokół, J. M., Kucharek, H., Baliukin, I. I., Fahr, H., Izmodenov, V. V., Kornbleuth, M., et al. (2022). Interstellar neutrals, pickup ions, and energetic neutral atoms throughout the heliosphere: present theory and modeling overview. *Space Sci. Rev.* 218, 18. doi:10.1007/s11214-022-00883-6

Sokół, J. M., McComas, D. J., Bzowski, M., and Tokumaru, M. (2020). Sun-heliosphere observation-based ionization rates model. *ApJ* 897, 179. doi:10.3847/1538-4357/ab99a4

Swaczyna, P., McComas, D. J., Zirnstein, E. J., Sokół, J. M., Elliott, H. A., Bzowski, M., et al. (2020). Density of neutral hydrogen in the sun's interstellar neighbourhood. *ApJ* 903, 48. doi:10.3847/1538-4357/abb80a

Thomas, G. E. (1978). The interstellar wind and its influence of the interplanetary environment. *Annu. Rev. Earth Planet. Sci.* 6, 173. doi:10.1146/annurev.ea.06.050178.001133

Usmanov, A. V., Matthaeus, W. H., Breech, B. A., and Goldstein, M. L. (2011). Solar wind modeling with turbulence transport and heating. *ApJ* 727, 84. doi:10.1088/0004-637X/727/2/84

Wang, B., Zank, G. P., Shrestha, B. L., Kornbleuth, M., and Opher, M. (2023). Relating energetic ion spectra to energetic neutral atoms. *ApJ* 944, 198. doi:10.3847/1538-4357/acb437

Wang, B. B., Zank, G. P., Adhikari, L., and Zhao, L. L. (2022). On the conservation of turbulence energy in turbulence transport models. *ApJ* 928, 176. doi:10.3847/1538-4357/ac596e

Williams, L. L., and Zank, G. P. (1994). Effect of magnetic field geometry on the wave signature of the pickup of interstellar neutrals. *J. Geophys. Res.* 99, 19229–19244. doi:10.1029/94JA01657

Zank, G., Matthaeus, W., Bieber, J., and Moraal, H. (1998). The radial and latitudinal dependence of the cosmic ray diffusion tensor in the heliosphere. *J. Geophys. Res. Space Phys.* 103, 2085–2097.

Zank, G., Matthaeus, W., and Smith, C. (1996). Evolution of turbulent magnetic fluctuation power with heliospheric distance. *J. Geophys. Res. Space Phys.* 101, 17093–17107.

Zank, G. P., Adhikari, L., Hunana, P., Shiota, D., Bruno, R., and Telloni, D. (2017). Theory and transport of nearly incompressible magnetohydrodynamic turbulence. *ApJ* 835, 147. doi:10.3847/1538-4357/835/2/147

Zank, G. P., Adhikari, L., Hunana, P., Tiwari, S. K., Moore, R., Shiota, D., et al. (2018). Theory and transport of nearly incompressible magnetohydrodynamic turbulence. IV. Solar coronal turbulence. *ApJ* 854, 32. doi:10.3847/1538-4357/aaa763

Zank, G. P., Dosch, A., Hunana, P., Florinski, V., Matthaeus, W. H., and Webb, G. M. (2012). The transport of low-frequency turbulence in astrophysical flows. I. Governing equations. *ApJ* 745, 35. doi:10.1088/0004-637X/745/1/35

Zank, G. P., Sterken, V., Giacalone, J., Möbius, E., von Steiger, R., Stone, E. S., et al. (2022). The early history of heliospheric science and the spacecraft that made it possible. *Space Sci. Rev.* 218, 34. doi:10.1007/s11214-022-00900-8

Zhao, L. L., Adhikari, L., Zank, G. P., Hu, Q., and Feng, X. S. (2018). Influence of the solar cycle on turbulence properties and cosmic-ray diffusion. *ApJ* 856, 94. doi:10.3847/1538-4357/aab362